Proceedings of the
Annual Stability Conference
Structural Stability Research Council
Orlando, Florida, April 12-15, 2016

Lateral Torsional Buckling of Welded Wide Flange Beams

Md. Imran Kabir[1], Anjan K Bhowmick [2]

Abstract
Lateral Torsional Buckling (LTB) can be defined as a combination of lateral displacement and twisting due to an application of load on an unsupported beam. Design specifications in North America (AISC 2010 and CSA S16-09) provide solutions for LTB of welded and rolled beams that were derived for constant moment situation. Same equations have been used over the years for design of rolled and welded shape beams. A recent study has shown that the current code equations might overestimate the capacity of the welded wide shape beams, which make them unsafe to use. Thus a detailed study is required to evaluate the existing LTB equations for welded wide flange (WWF) shapes. This paper evaluates the performance of current equations in providing LTB capacities of WWF shape beams. A nonlinear finite element (FE) model is developed using the commercial finite element software ABAQUS. In total 75 FE model for 15 WWF shape beams are analysed. For the FE analysis, the beams are considered simply supported beams with uniform moments applied at the ends. Initial residual stresses in the WWF shapes that are reported in the literature are also included in the FE model.

Keywords: Lateral torsional buckling, unsupported beam, welded section, finite element model

1. Introduction

Lateral torsional buckling (LTB) is a state of buckling where a member exhibits both deflection and twisting as shown in Fig.1. Usually flexural member such as beams and girders have much greater strength about the major axis compared to minor axis. As a result of this, laterally unsupported beams and girders might fail by lateral-torsional buckling before the attainment of their full in-plane capacity. So, lateral–torsional buckling can be considered as a limit state of structural design where the deformation changes from predominantly in-plane bending to combined lateral deflection and twisting (Ziemian 2010). The final failure pattern involves lateral deflection and twisting in combination with various extents of yielding and flange and/or web local buckling depending on the specific member characteristics (Ziemian 2010).

The main variable affecting the capacity of LTB is unbraced length of member. Depending on this length behaviour of LTB can be divided into three parts such as (1) elastic buckling, (2)

[1] Graduate Research Assistant, Concordia University, <md_kabi@encs.concordia.ca>
[2] Assistant Professor, Concordia University, <anjan.bhowmick@concordia.ca>

inelastic buckling and (3) plastic behaviour. The relationship between critical moment (M_{cr}) and unbraced length (L) for lateral-torsional buckling can be presented graphically as Fig.2.

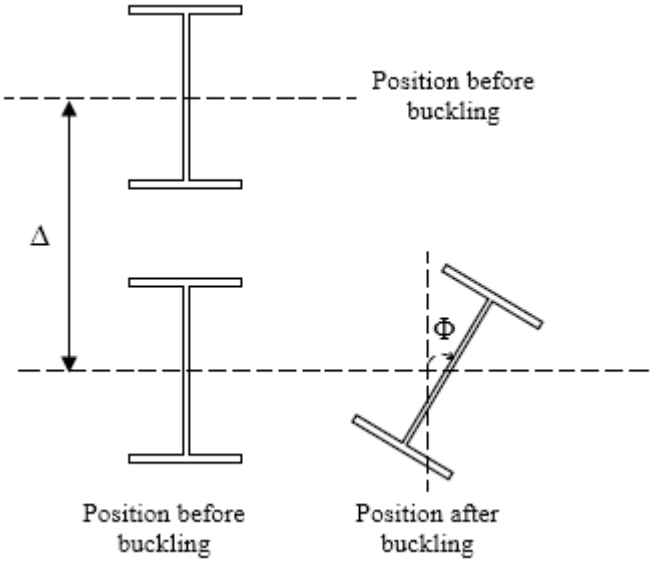

Figure 1: Lateral torsional buckling

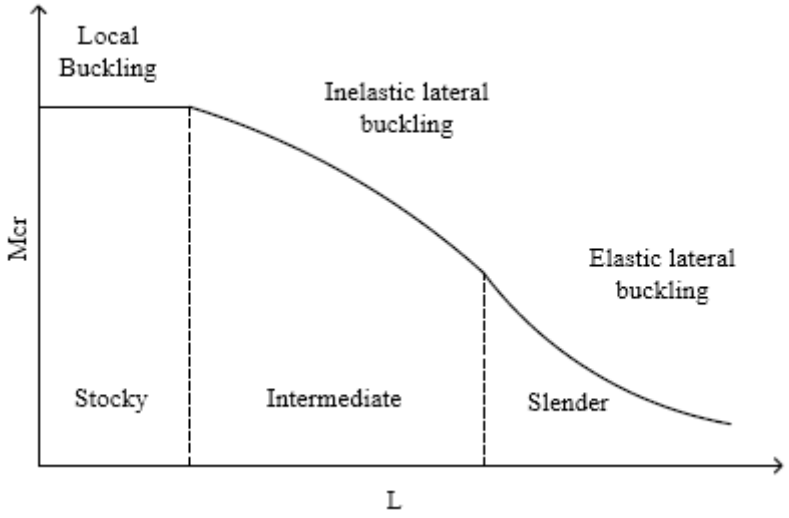

Figure 2: Failure modes of beam

Different structural steel design standards (e.g., CAN-CSA S16-09 (2009), AISC-ANSI 360-10 (2010), AS 4100 (1998) , and Eurocode 3 (2005)) provide different algebric equations for estimating the LTB resistance. However, in a general sense, all of them use similar approach: staring from the calculation of elastic LTB resistance M_e and followed by a reduction of this theoretical resistance by considering various factors such as geometric imperfections, local and/or distorsional buckling, residual stress etc. (Ziemian 2010). Depending on the variables considered, nominal resistance for LTB varies considerably from statndard to standard. Australian and the European standards, AS 4100 and EC 3, provide a substantial penalty for

geometric imperfections (Ziemian 2010). Another important difference between Eurocode 3 and other standards is Eurocode 3 provides two different strength curves for rolled and welded section. However, two North American standards AISC 2010 and CSA S16-09 implicitly assume that the beam has no initial out-of-straightness for long members that fail by elastic LTB. (Ziemian 2010). Moreover both AISC 2010 and CSA S16-09 make no distinction between rolled and welded beams. The Canadian CSA S16-09 strength curve (CSA 2009) for doubly symmetric Class 1 and 2 sections can be defined using equations (1-3)

$$M_e = \frac{\Pi}{L_u}\sqrt{EI_y GJ + \left(\frac{\Pi E}{L_u}\right)^2 I_y C_w} \tag{1}$$

$$M_r = \phi M_e \le \phi M_p \text{ if } M_e \le 0.67 M_p \tag{2}$$

$$M_r = 1.15\phi M_p\left(1-\frac{0.28M_p}{M_e}\right) \le \phi M_p \text{ if } M_e > 0.67 M_p \tag{3}$$

where M_e is the elastic moment, M_p is the full plastic moment of section, M_r is the factored resistance, L_u is the unbraced length of beam, E is modulus of elasticity, I_y is moment of inertia in weak axis, G is shear modulus of elasticity, J is Saint-Venant torsion constant and C_w is warping constant.

2. Literature Review

Since the mid-nineteenth century, research has been performed intensively on lateral torsional buckling of beams and reported in several text books (Bleich 1952; Timoshenko and Gere 1961; Vlasov 1961; Galambos T. 1968; Trahair 1993). Several test on lateral torsional buckling of I-beams were also carried out on hot rolled and welded section by many researchers. Among them, Galambos (1963) was the first who considered the effect of residual stress to investigate the inelastic buckling behavior of beam. A series of experimental test was also conducted by Dibley (1969) on rolled beams of universal I-section for grade 55 steel. Four point loading test was performed to achieve a uniform moment situation for center portion of beam. Residual stress measurements were done on both surfaces of flanges and web of the beam. Maximum moment capacity of test beams were reported. Later on, Fukumoto et al. (1971) investigated the lateral buckling behavior and reported the strength of the flexural members of high strength steel. Both welding and annealing condition were assumed to obtain the test results. The test results were also compared with the theory for the specified residual stress pattern and initial imperfection. In addition, Fukumoto and Kubo (1977) made a review on experiments conducted for lateral buckling of beams and girders. The purpose of this review was to gather strength data from several experiment conducted on laterally supported and unsupported beams which failed by lateral buckling. Fukumoto et al. (1980) included initial imperfection i.e. residual stress and initial out of straightness into twenty five laterally unsupported beam specimens and performed an experimental investigation to observe the strength variation of those beams. A concentrated point load was applied at the top flange and different level of initial imperfections were considered. Another statistical study was presented for the experiment of laterally unsupported welded beams by Fukumoto and Kubo (1981). The measured value of longitudinal residual stress was significantly large compared to rolled beams in those experiment. Also, the ultimate moment capacity was much lower for welded section compared to rolled section of similar geometry. Baker and Kennedy (1984) conducted a statistical analysis on the test results of Dibley (1969) to

determine the resistance factor for laterally unsupported beam. The proposed resistance factor from this analysis had been adopted by CSA S16-09. Also a recent reliability analysis conducted by MacPhedran and Grondin (MacPhedran 2009) showed that current code might overestimate the capacity for welded wide flange beams. It was recommended that a comprehensive study must be conducted to evaluate performance of the current code formula in estimating strength of WWF sections due to LTB. Thus, the purpose of this paper is to investigate the LTB capacity of WWF beams when subjected to uniform bending moment along the full length of the beams. For this purpose, a finite element model is developed using the commercial finite element (FE) software ABAQUS for the nonlinear inelastic analysis of welded wide flange beams with a wide range of unbraced length. The FE model is then used to evaluate the performance of current CSA S16-09 approach in predicting the moment capacity of laterally buckled welded wide flange beams with various unbraced span lengths.

3. Nonlinear Finite Element Modeling

To simulate the behavior of a steel beam (WWF section) that undergoes LTB due to an application of uniform end moment, a nonlinear inelastic finite-element model is developed based on the specifications and assumptions given in the following sections.

3.1 Elements and Mesh Configuration

A nonlinear FE model is developed using the commercial finite element software package ABAQUS (ABAQUS 2010). Both geometric and material nonlinearities are included in the finite element model. Shell element is the most widely used element for complex buckling behaviour and can be referred as a suitable element because of its capability of providing accurate solutions in case of a structure whose thickness is much smaller than the other dimensions (Smalberger 2014). Apart from that, conventional shell elements have six DOFs per node: three translation DOFs and three rotational DOFs per node. For this reason, a 4-node doubly curved shell with reduced integration S4R (ABAQUS 2010) element has been chosen from ABAQUS element library to model the web and flanges of the WWF sections. Element type S4R accounts for finite membrane strains and arbitrary large rotations which makes them suitable for large-strain analysis (ABAQUS 2010).

Simplicity of the geometry of this model makes the mesh configuration very easy. The element shape is quad-dominated and adequate mesh density has been achieved for the section with 8 elements across the width of flange and 32 elements along the height of web as shown in Fig 3. This configuration of the mesh was obtained from a mesh sensitivity analysis. Steel material was modelled with bilinear isotropic hardening and elastic perfectly plastic strain stress property. A typical value of modulus of elasticity, $E = 200{,}000\,MPa$, nominal yield stress, $F_y = 350\,MPa$ and Poison's ratio of 0.3 was used in this study.

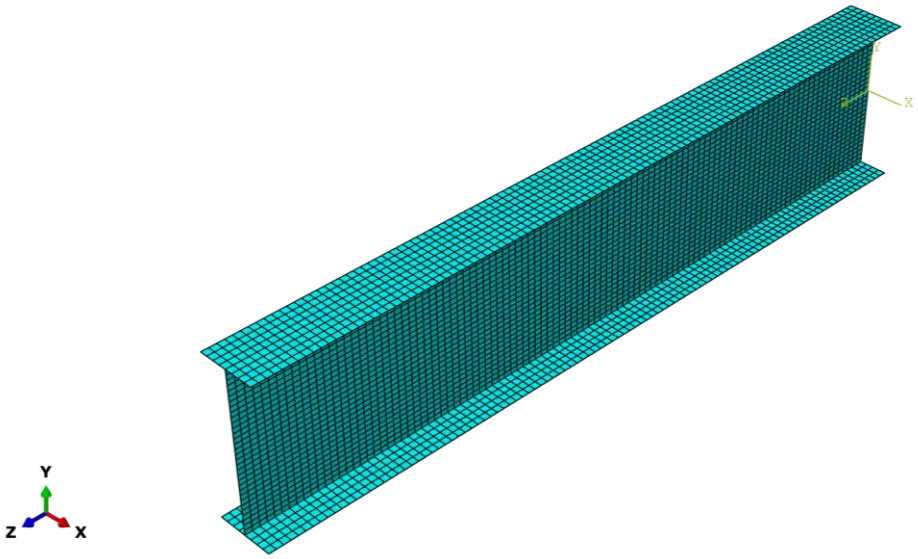

Figure 3: Mesh configuration of finite element model

3.2 Boundary Conditions

The beams considered in this study are simply supported at both ends relative to the strong axis bending, weak axis bending, and twist. It is essential to confirm that idealized boundary conditions adopted in modelling are as close as possible to theoretical buckling analysis. Hence, theoretical simply support boundary conditions given by Trahair (1993), has been replicated into this model by means of the following criterion.

1. Simply supported in plane: centroids of both ends were restrained against in-plane y-axis deflection $(U_2 = 0)$ but unrestrained against in-plane rotation $(UR_1 \neq 0, UR_2 \neq 0)$, also one end was restrained against z-axis displacement $(U_3 = 0)$.

2. Simply supported out-of-plane: all web nodes including the centroid of both ends were restrained against out-of-plane x-axis deflection $(U_1 = 0)$ and only centroids of the both ends were restrained against z-axis rotation $(UR_3 = 0)$, but unrestrained against minor axis rotation and warping displacement (Trahair 1993).

In conjunction with the above criterion, nodes of the cross section at both ends are constrained to simulate the theoretical simply supported boundary conditions successfully as depicted earlier using the following equation proposed by (Xiao 2014).

$$w(l_e, x, y) - \begin{pmatrix} 1 & x & y & xy \end{pmatrix}^T \begin{pmatrix} 1 & x_1 & y_1 & x_1 y_1 \\ 1 & x_2 & y_2 & x_2 y_2 \\ 1 & x_3 & y_3 & x_3 y_3 \\ 1 & x_4 & y_4 & x_4 y_4 \end{pmatrix}^{-1} \begin{Bmatrix} w_1 \\ w_2 \\ w_3 \\ w_4 \end{Bmatrix} = 0 \tag{4}$$

Equation (4) provides longitudinal displacement w of any characteristic nodal point of end cross-section in terms of longitudinal displacement of four corner points (Xiao 2014). Using this equation, corresponding longitudinal displacement of four corner points for all nodal points (except the center node of web of both end) of end cross-section of both ends are calculated and enforced in ABAQUS using the equation constraint feature (ABAQUS 2010) as shown in Fig.4.

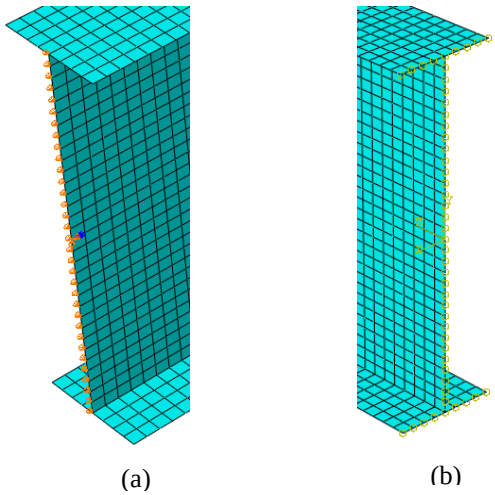

Figure 4: (a) Boundary condition (Pin End), (b) Applied equation constraint (Roller End)

3.3 Load Application

As discussed earlier, CSA S16-09 equation was derived for constant moment situation. In ABAQUS, uniform end moment condition is obtained by applying concentrated force on four corner point as shown in Fig.5. Thus, the magnitude of concentrated force is determined to apply a uniform moment of $1 kNm$. Similar method for applying uniform moment was followed earlier by several researchers in different analytical model (Xiao 2014; Hassan 2013; Amin Mohebkhah 2012; Sharifi 2015).

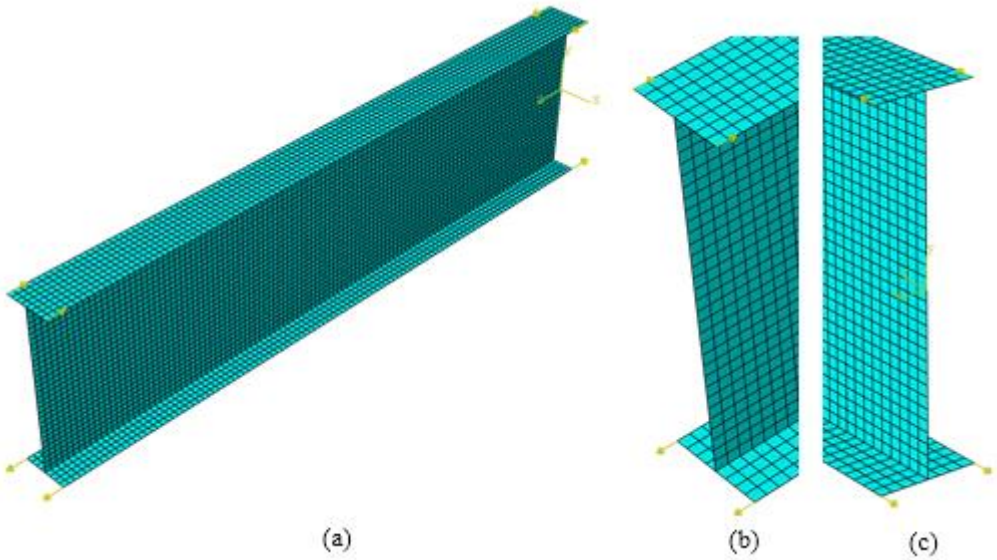

Figure 5: Loading scheme (a) whole model, (b) left end and (c) right end

3.4 Analysis Type

Two types of analysis i.e. elastic buckling analysis and non-linear analysis are conducted to estimate the ultimate load carrying capacity of beams subjected to pure bending loading configuration as specified above. Firstly, an eigenvalue analysis is performed for elastic buckling analysis in which eigenvalues of corresponding eigenmodes are requested using the linear perturbation buckling analysis. In this study, four eigenvalues for each run were extracted. From the eigenvalue analysis a suitable pattern of imperfection is obtained and incorporated into non-linear analysis.

A RIKS analysis is selected to do the nonlinear post buckling analysis since this technique is usually suitable for predicting the instability as well as for understanding the non-liner behavior of geometric collapse (ABAQUS 2010). RIKS method is based on Arc-length method, a form of Newton-Raphson iteration method, in which an additional unknown named load proportionality factor is introduced to provide solutions concurrently for load and displacement.

3.5 Geometric Imperfection and Residual Stress

According to Trahair (1993), the lowest eigenvalue refers the load which initiates the buckling of a structure and associated eigenvector refers the related buckling shape or buckling mode of that structure. Therefore, buckling mode obtained from the lowest positive eigenvalue from eigenvalue buckling analysis is chosen to determine the buckled shape. But, it would be worthy to mention that buckling mode shapes do not predict the actual deformation magnitudes rather they are normalized to provide the maximum displacement value as 1.0. So, the first buckling mode shape must be scaled with a suitable factor to take account the effect of imperfection on LTB. Column strength curves from SSRC (Bjorhovde 1972) were developed using L/1000 as maximum permissible initial out-of-straightness. In addition, two North American structural steel delivery specifications (e.g., ASTM A6 in the United States; CSA G40.20 in Canada) restrict the magnitude of maximum initial out-of-straightness as a factor of L/1000 (Ziemian 2010). However, Chernenko and Kennedy (1991) reported a relatively less initial crookedness with a mean value of approximately L/3300 for welded wide flange shapes. In this study, a maximum initial out-of-straightness of L/2000 is assumed as an initial condition.

Both magnitude and distribution of residual stress will be considerably different due to welding as reported by various research (Alpsten and Tall 1970; Nethercot 1974; Fukumoto 1981). Results from different experiments showed that residual stress can be dependent on few parameter such as manufacturing processes, geometry of the section, fabrication process etc. (McFalls and Tall 1969; Alpsten and Tall 1970). However, weld type and yielding strength of material do not show any significant effect on magnitude and distribution of residual stress (Alpsten and Tall 1970). Typical residual stress pattern had also been suggested by (Chernenko and Kennedy 1991) as shown in Fig. 6 and these were based on a number of experimental values of residual stress as presented in literature. For the pupose of this study, a simple residual stress pattern similar to typical residual stress pattern for WWF-universal mill plate is asuumed as depicted in Fig. 6. Maximum compressive and tensile residual stress are taken as 0.3Fy and 0.5Fy which is equal to the measured experimental value of welded shape of 15H290-universal mill plates (14’’x10’’x2.5’’x1.5’’) of A36 and A441 steel for two types of weld namely fillet and groove weld by Alpsten and Tall (1970). In FE model, the residual stresses are specified directly

using the predefined field feature of ABAQUS as initial stress. A static step is also defined prior to RIKS analysis for the equilibrium of residual stress. No load is applied during this step.

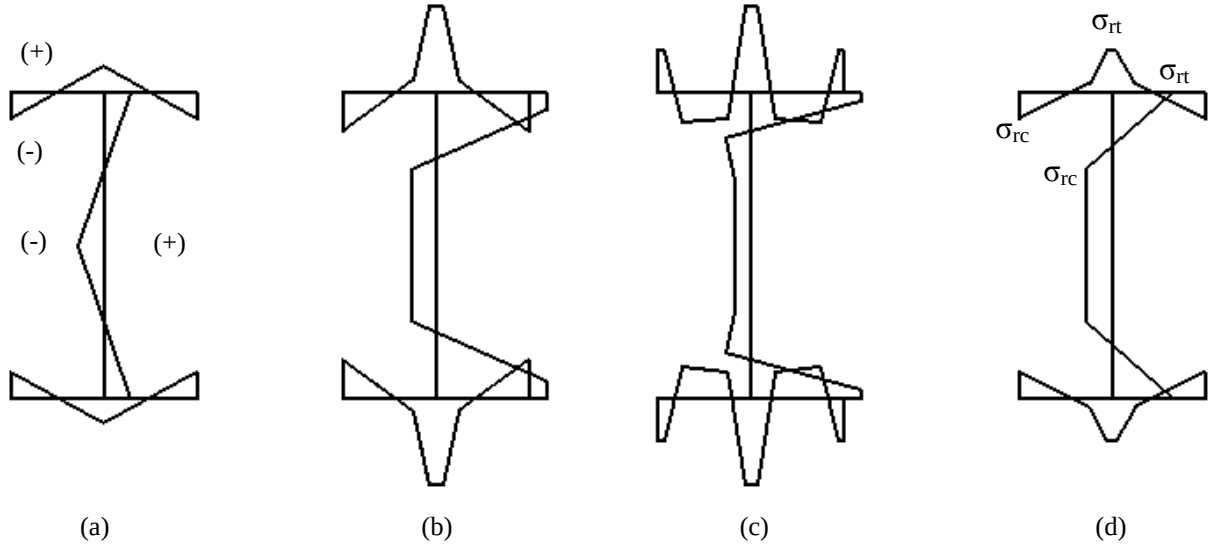

Figure 6: Typical residual stress pattern (a) hot rolled, (b) WWF-universal mill plate, (c) WWF-flame cut, (Chernenko and Kennedy 1991) & (d) assumed residual stress pattern for FEM

3.6 Validation of Finite Element Model

As stated earlier, Canadian CSA S16-09 strength curve (CSA 2009) for doubly symmetric Class 1 and 2 sections is based on a statistical analysis conducted by Baker and Kennedy (1984). This analysis was done from the test result of rolled I-section member test which had been performed by Dibley (1969). In total 30 tests were done on five universal beam section for different unbraced length. Four-point loading was used in order to consider the center portion of beam as an unsupported beam carrying a uniform moment. Reported effective length factor was from 0.55 to 0.7. So, to validate the finite model developed in this study, the effective length used in the test was selected and uniform moment of 1kN-m was applied. In addition, residual stress for the tested sections as reported in experimental calculation was also applied in FE model and comparison is shown in Fig. 7. Results from the non-linear FE analysis is compared with the experiment results as shown in Table 1.

Table 1: Comparison of FEM result with test result

Section	d (mm)	b (mm)	t (mm)	w (mm)	L (m)	Efective Length Factor	Effective Length	Moment (exp) kN.m	Fy (MPa)	E (Mpa)	Moment (FEM) kN.m	% Error
12x4 UB 19	308.9	101.9	8.9	6.1	3.77	0.7	2.64	105.9	516	206000	102.6	3.12
					3.29	0.7	2.30	126.3			119.87	5.09
					2.09	0.7	1.46	190			192.19	-1.15
					1.05	0.7	0.74	226.1			231.08	-2.20
					1.47	0.7	1.03	204.6			207.32	-1.33

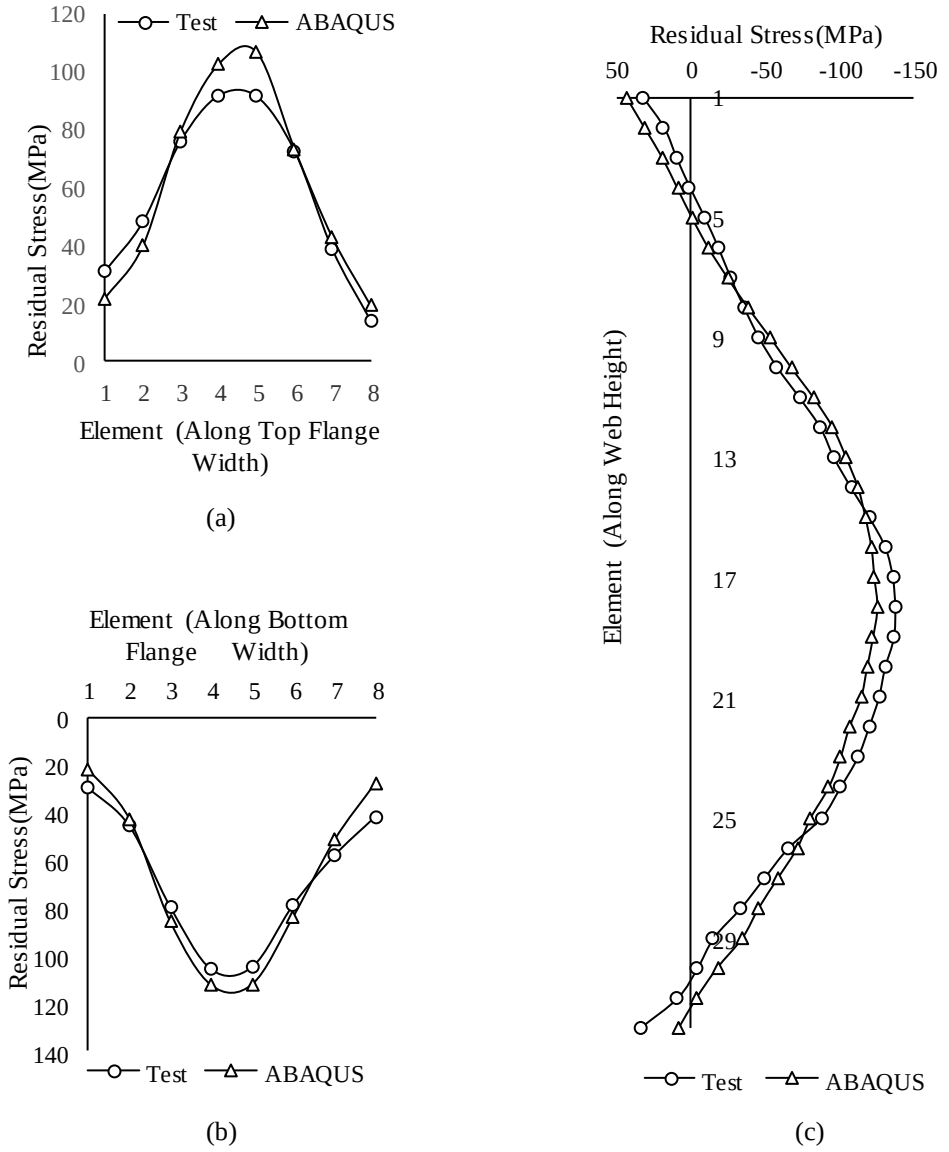

Figure 7: Pattern of residual stress from ABAQUS & test (a) top flange, (b) bottom flange, and (c) web

4. Design of Parametric Study

The validated FE model is used to investigate the LTB moment resisting capacity of welded wide flange section under uniform end moment condition. For this purpose, a wide range of dimensionless slenderness ratio (L/r_y) from 57.97 to 225 is selected so that the beams lie both in elastic and inelastic region. Selected beam depth, flange width, flange thickness and web thickness vary between 1800mm-700mm, 300mm-550mm, 50mm-25mm and 11mm-20mm respectively.

For the parametric study, 15 cross sections of WWF shape with different length are selected with an aim to estimate their moment resisting capacity due to LTB in different behavioral regions. In total 75 FE models are developed. Table 2 presents the ultimate moment capacities $Mu\,(FEM)$ obtained from FE analysis along with the values estimated from the equation provided in CSA S16-09. Differences between the predicted capacity and the code values are also reported.

Table 2: Results from parametric study

Section	Moment (kN-m)	Length (m)												
		6	6.5	7	7.5	8	9	10	11	12	14	16	18	20
WWF 1800x700	Mfem*				13900		12208		11132		8853			5583
	Mcode*				21778		20333		18111		14222			7911
	%difference				36.2		40.0		38.5		37.8			29.4
WWF 1800x510	Mfem*			9496		8575		7853			5453		3770	
	Mcode*			13778		12888		10833			6144		3922	
	%difference			31.1		33.5		27.5			11.2		3.9	
WWF 1400x597	Mfem*					11150		10056		9062		7100		5545
	Mcode*					15333		14111		12778		9567		6822
	%difference					27.3		28.7		29.1		25.8		18.7
WWF 1400x405	Mfem*		6975				6036			4820		3443		2498
	Mcode*		9711				8422			6444		3856		2656
	%difference		28.2				28.3			25.2		10.7		5.9
WWF 1200x487	Mfem*						8014		6649		5648	4980		3895
	Mcode*						10178		9244		7678	6411		4544
	%difference						21.3		28.1		26.4	22.3		14.3
WWF 1200x418	Mfem*			6560		6340			5073		4100			2670
	Mcode*			8878		8478			7033		5222			2967
	%difference			26.1		25.2			27.9		21.5			10.0
WWF 1200x380	Mfem*			5785			5129		4671	4104			2531	
	Mcode*			7844			7033		6078	5556			2844	
	%difference			26.2			27.07		23.15	26.1			11.0	
WWF 1100x458	Mfem*					6985		6764		6096		4603		3600
	Mcode*					9444		8722		7911		6056		4322
	%difference					26.0		22.4		22.9		24.0		16.7
WWF 1000x447	Mfem*						5987	5790	5420		4672		3792	
	Mcode*						8178	7867	7533		6467		4822	
	%difference						26.8	26.4	28.0		27.8		21.4	
WWF 1000x262	Mfem*	3431		2895				2348		1787			1059	
	Mcode*	4344		4044				2944		2144			1122	
	%difference	21.0		28.4				20.2		16.7			5.6	
WWF 900x417	Mfem*						5203		4903		4572		3710	3050
	Mcode*						7111		6611		5789		4567	3944
	%difference						26.8		25.8		21.0		18.8	22.7
WWF 900x347	Mfem*					4263	4049			3391		2675		2096
	Mcode*					5833	5589			4778		3500		2544
	%difference					26.9	27.6			29.0		23.6		17.6
WWF 800x339	Mfem*					3745		3409	3226		2754		2233	
	Mcode*					5122		4711	4500		3822		2811	
	%difference					26.9		27.6	28.3		27.9		20.6	
WWF 700x245	Mfem*	2375		2229			1964			1601			975	
	Mcode*	3211		3056			2711			2167			1244	
	%difference	26.0		27.1			27.6			26.1			21.6	
WWF 700x175	Mfem*	1500		1228		1102				715.8			455	
	Mcode*	1889		1700		1500				823			484	
	%difference	20.59		27.76		26.53				13.03			5.99	

* Values are rounded to the nearest 1.0

5. Discussion on Results from Parametric Study

Results from FE analysis can be summarized in three sections: a) comparison of analytical results with code, b) load-deflection behavior and c) yielding behavior of beam.

5.1 Comparison of Analysis Results with CSA S16-09:

Prior to compare the analysis results with CSA S16-09 strength curve, the results are to be non-dimensionalized. For this purpose, ultimate moment capacity for LTB, M_u from both FE and CSA S16-09 equations are non-dimensionalized by the plastic moment of corresponding section, M_p. Also, a modified slenderness ratio, $\lambda = \sqrt{M_p / M_e}$, where M_e is the elastic moment capacity of beam using equation (1) is used. Thus, Fig. 8 shows a presentation of CSA S16-09 strength curve along with the FE analysis result obtained from ABAQUS on the plot M_u / M_p vs $\sqrt{M_p / M_e}$, where M_u refers to ultimate moment capacity from both FE analysis and CSA S16-09 equations.

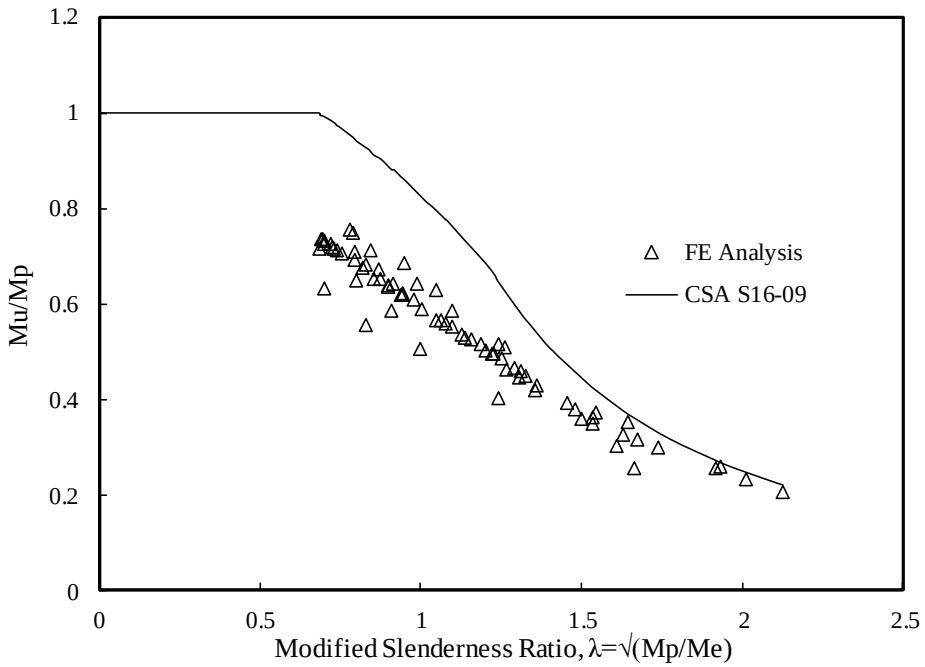

Figure 8: Comparison of finite element analysis result with CSA S16-09 equation

5.2 Load-Deflection Behavior of Beam

The behavior of load versus horizontal and vertical deflection is depicted in Fig. 9 for beams with four different slenderness ratios for the WWF1400x405 section. Similar pattern of load-versus-horizontal and vertical deflection curves are achieved for other sections. The ordinate corresponds to M_u / M_p, where M_u = computed moment capacity from ABAQUS due to LTB and M_p = plastic moment of the section. Since initial geometric imperfection of amount L/2000 is incorporated to each beam, horizontal deflections of both compression flange, U_c, and tension

flange, U_t, increase gradually up to the point where instability occurs. Then this curves dips sharply due to considerable reduction in stiffness. Also, the increment rate of vertical deflection after the instability is very steady compare to initial rate.

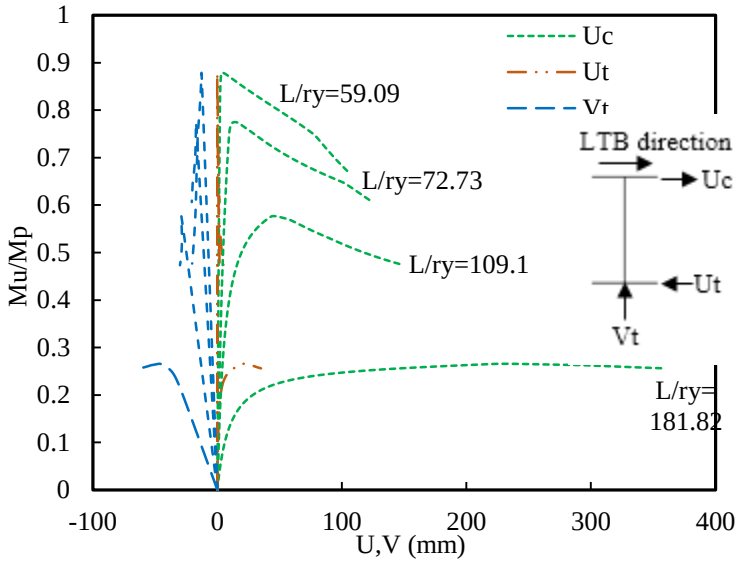

Figure 9: Load-deflection curve of WWF 1400x405 for different L/ry

5.3 Yeilding Behavior of Beam

The yielding behavior of beam due to the inclusion of residual stress in beams can be well understood from Fig. 10. As it is seen from Fig. 10a, web to bottom flange junction region yields first. This tensile yielding imposes very insignificant effect on section's stiffness and thus decreases the moment capacity of beam slightly as suggested by Nethercot (1974). After that, outer part of compression flange i.e. top flange starts (Fig. 10c) to yeild with the increment of loading. This yeilding phenomena causes rapid decrease in section's stiffness which in turns creates inslability to beams reffering that member is not capable of carrying any further load. The moment capacity which has been reported in Table 1 from FEM also refers the moment applied at this increment. Eventually yeilding starts to propagate along the web (Fig. 10d) and local buckling occurs in different part of the member. The continous yeilding of web is the main reason to make a section almost completely strain hardened which consequently possibles the attainment of full plastic moment, M_p for adequately short span beams Nethercot (1974).

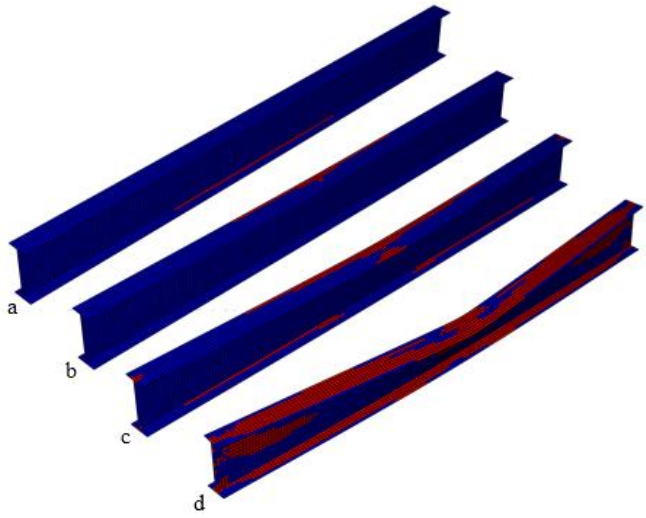

Figure 10: Yeilding pattern of member in ABAQUS at (a) 15th, (b) 22nd, (c) 27th and (d) 35th increment

6. Conclusions

A nonlinear FE model is developed for studying the lateral torsional buckling capacity of welded wide flange beams. The FE model is validated against the test results from a rolled I beam subjected to uniform bending moment along the length. Inelastic lateral torsional buckling analysis of a series of WWF shape beams with a wide range of unbraced length and slenderness ratio is carried out for uniform moment condition. It was observed from FE analysis that, CSA S16-09 approach is somewhat unconservative for intermediate WWF beams failing in inelastic LTB compared to slender e beams. The difference between FE and code results were large for beams within the inelastic range and becomes small as it goes to elastic range. In addition, it showed more discrepancies in case of deep beam than shallow one. It should be noted that a limited number of beams are analysed in this study. In addition, a simplified residual stress pattern is assumed for this study. Thus, the above conclusions must be considered with caution. Since residual stress pattern and magnitude vary due to section geometry, manufacturing and fabrication processes, further analytical and experimental investigations need to be carried out with different residual stress patterns and magnitudes to have a critical evaluation of current CSA S16-09 approach for estimating LTB capacity of welded wide flange beams. In addition, the code equation must be evaluated for other moment gradient situation which is currently in progress.

ACKNOWLEDGEMENTS

Funding for this research project is provided by the Canadian Institute of Steel Construction. The authors gratefully acknowledge Dr. Gilbert Y. Grondin for his valuable suggestions in this project.

References

ABAQUS. (2010). *ABAQUS standard user's manual, 6.11.* Dassault Systèmes.

Alpsten, G., & Tall, L. (1970). Residual stresses in heavy welded shapes. *Welding Journal, Research Supplement, 49(3)*, 93s- 105s.

American Institute of Steel Construction (AISC). (2010). *Specification for Structural Steel Buildings, ANSI/AISC 360-10,*. Chicago, IL: AISC.

Amin Mohebkhah, & Chegeni, B. (2012). Local–global interactive buckling of built-up I-beam sections. *Thin-Walled Structures*, 33-37.

AS 4100. (1998 Steel Structures). *Standards Association of Australia,*. Sydney, Australia.

Baker, K. A. (1984). Resistance Factors for Laterally Unsupported. *Can. J. Civil Eng.*, 1008–1019.

Bjorhovde, R. (1972). *Deterministic and Probabilistic Approaches to the Strength of Steel Columns.* Ph.D. dissertation, Lehigh University, Bethlehem, PA.

Bleich, F. (1952). *Buckling Strength of Metal Structures.* McGraw-Hill, New York.

Canadian Standards Association, (CSA). (2009). *Limit States Design of Steel Structures.* CAN/CSA-S16-09: Toronto, Ontario, Canada.

Chernenko, D. E., & Kennedy, D. J. (1991). An Analysis of the Performance of Welded Wide Flange Columns,. *Can. J. Civil Eng., Vol. 18,*, pp. 537–555.

Dibley, J. E. (1969). Lateral Torsional Buckling of I-Sections in Grade 55 Steel. *Proc. Inst. Civil Eng.*, 599–627.

Eurocode 3. (2005). *EN 1993-1-1 Eurocode 3: Design of steel structures - Part 1–1: general rules and rules for buildings. European Committee for Standardization (CEN).* Brussels, Belgium.

Fukumoto, Y., & Itoh, Y. (1981). Statistical Study of Experiments on Welded Beams. *Journal of Structural Division, ASCE, 107 (ST1):*, 89-103.

Fukumoto, Y., & Kubo, M. (1977). An experimental review of lateral buckling of beams and girders. *International Colloquium on Stability of Structures Under static and Dynamic Loads, ASCE*, 541-562.

Fukumoto, Y., Fujiwara, M., & Watanabe, N. (May, 1971). Inelastic Lateral Buckling Tests on Welded Bemas and Girders. *Proceedings of the Japanese Society of CIvil Engineers, Paper 189*, 39-51.

Fukumoto, Y., Itoh, Y., & Kubo, M. (1980). Strength Variation of Laterally Unsupported Beams. *Journal of Structural Division, ASCE, 106 (ST1):*, 165-181.

Galambos, T. (1968). *Structural Members and Frames.* Prentice-Hall, Upper Saddle River, N.J.

Galambos, T. V. (1963). Inelastic Lateral Buckling of Beams. *ASCE J. Struct. Div, Vol.89, No. ST5*, 217-244.

Hassan, R. (2013). *Distortional Lateral Torsional Buckling Analysis for Beams of Wide Flange Cross-Sections.* M.A.Sc dissertation, Department of Civil Engineering, Faculty of Engineering, University of Ottawa, Canada.

MacPhedran, I., & Grondin, G. (2011). A Proposed Simplified Canadian Beam Design. *Can. J. Civ. Eng. 38:*, 141-143.

McFalls, R. K., & Tall, L. (1969). A study of welded columns manufactured from flame-cut plates. *Welding Journal, Research Supplement, 48(4)*, 141s- 153s.

Nethercot, D. (1974). Buckling of welded beams and girders. *IABSE publications*, 107-121.

Sharifi, S. T. (2015). Inelastic lateral-torsional buckling capacity of corroded web opening steel beams using artificial neural networks. *The IES Journal Part A: Civil & Structural Engineering*, 24-40.

Smalberger, H. J. (2014, December). *Comparative study of the equivalent moment factor between international steel design specifications.* Master of Science dissertation, Faculty of Engineering at Stellenbosch University, South Africa.

Timoshenko, S. P., & Gere, J. M. (1961). *Theory of Elastic Stability, 2nd ed.* McGraw-Hill, New York.

Trahair, N. S. (1993). *Flexural-Torsional buckling of structures.* CRC Press, Boca Raton, FL.

Vlasov, V. Z. (1961). *Thin- Walled Elastic Beams.* Israel Program for Scientific Translations, Jerusalem.

Xiao, Q. (2014, April). *Lateral Torsional Buckling of Wood Beams.* M.A.Sc dissertation, Departments of Civil Engineering, University of Ottawa, Canada.

Ziemian, Ronald D., Editor. (2010). *Guide to Stability Design Criterion for Metal Structures.* Hoboken, New Jersy: John Wiley & Sons, Inc.